

Studies on the selectivity mechanism of wild-type *E. coli* thioesterase 'TesA and its mutants for medium- and long-chain acyl substrates

Xinyue Zhang ¹, Hao Zhang ¹, Shanshan Guan ^{2,3}, Zhijian Luo ¹, Jingwen E ¹, Zhijie Yang ¹, Juan Du ¹ and Song Wang ^{1,*}

¹ Institute of Theoretical Chemistry, College of Chemistry, Jilin University, Changchun 130023, China

² College of Biology and Food Engineering, Jilin Engineering Normal University, Changchun 130052, China

³ Key Laboratory of Molecular Nutrition at Universities of Jilin Province, Changchun 130052, China

*Correspondence: ws@jlu.edu.cn (S.W.); Tel.: +86-0431-88498761

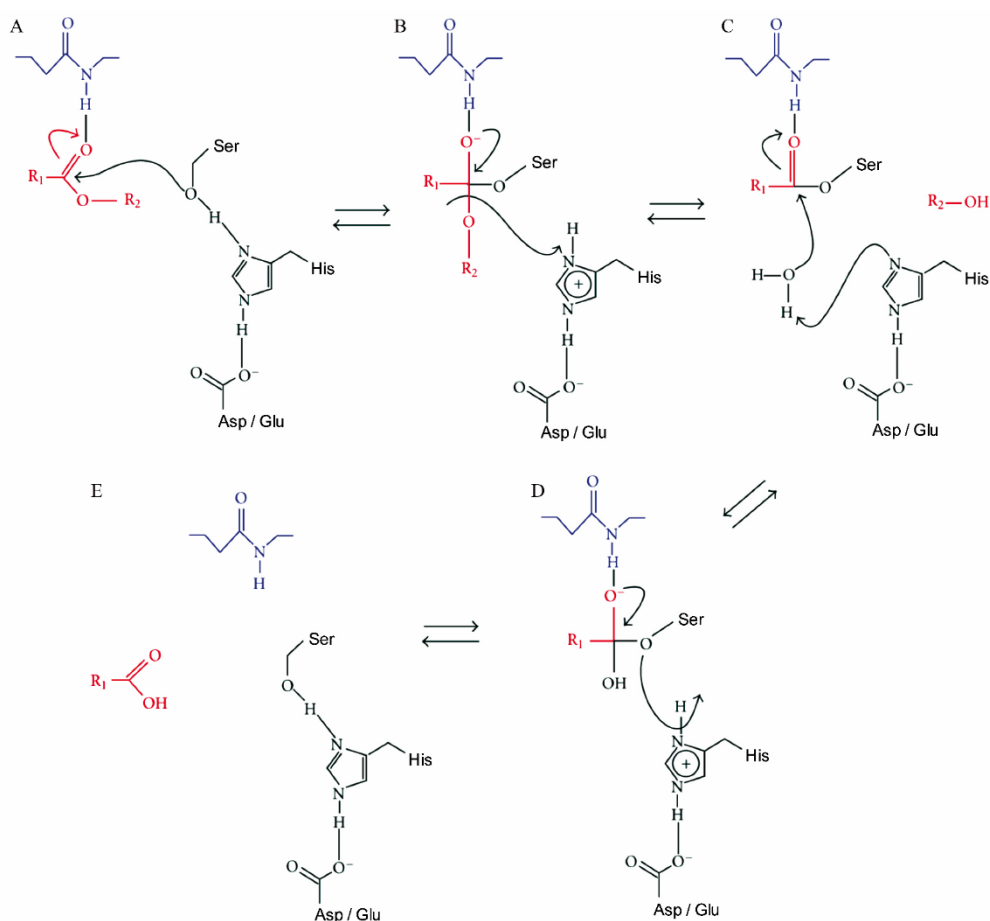


Figure S1. Catalytic mechanism of *E. coli* thioesterase. Catalytic triplets and water molecules are represented in black, oxygen anion holes in blue, and substrates in red.

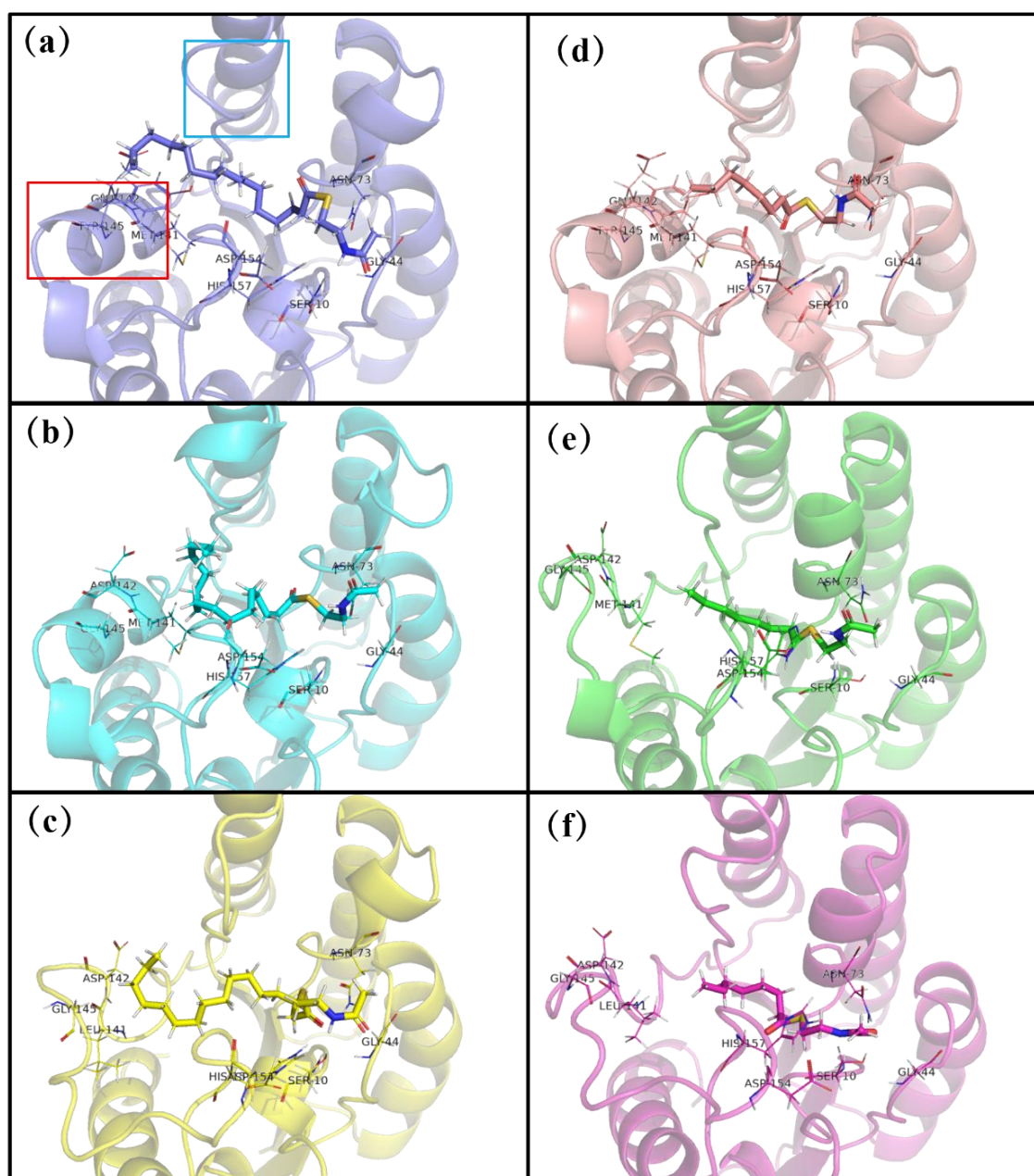


Figure S2. Initial docking conformation diagrams of the six complexes. (a) 'TesA_C16-SNAC, (b) 'TesA^{E142D/Y145G}_C16-SNAC, (c) 'TesA^{M141L/E142D/Y145G}_C16-SNAC, (d) 'TesA_C8-SNAC, (e) 'TesA^{E142D/Y145G}_C8-SNAC, (f) 'TesA^{M141L/E142D/Y145G}_C8-SNAC. Proteins are represented by solid-ribbon, substrates by stick and important residues by line.

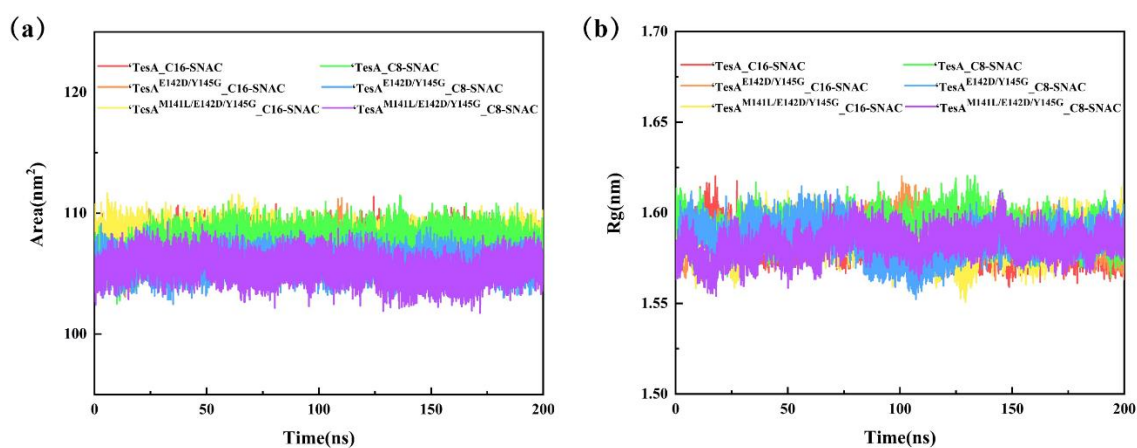


Figure S3. (a) Solvent Accessible Surface Area (SASA) values for the six complexes during the 200 ns MD simulation. (b) Radius of Gyration (Rg) of the six complexes as a function of simulation time.

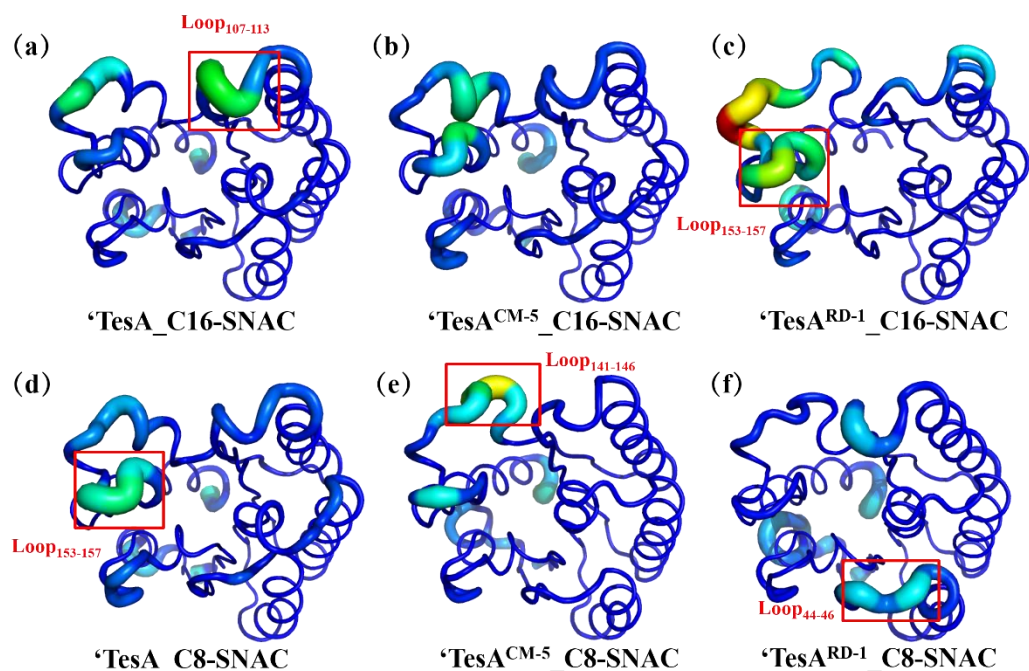


Figure S4. Visualizations of the backbone flexibility for the six complexes.

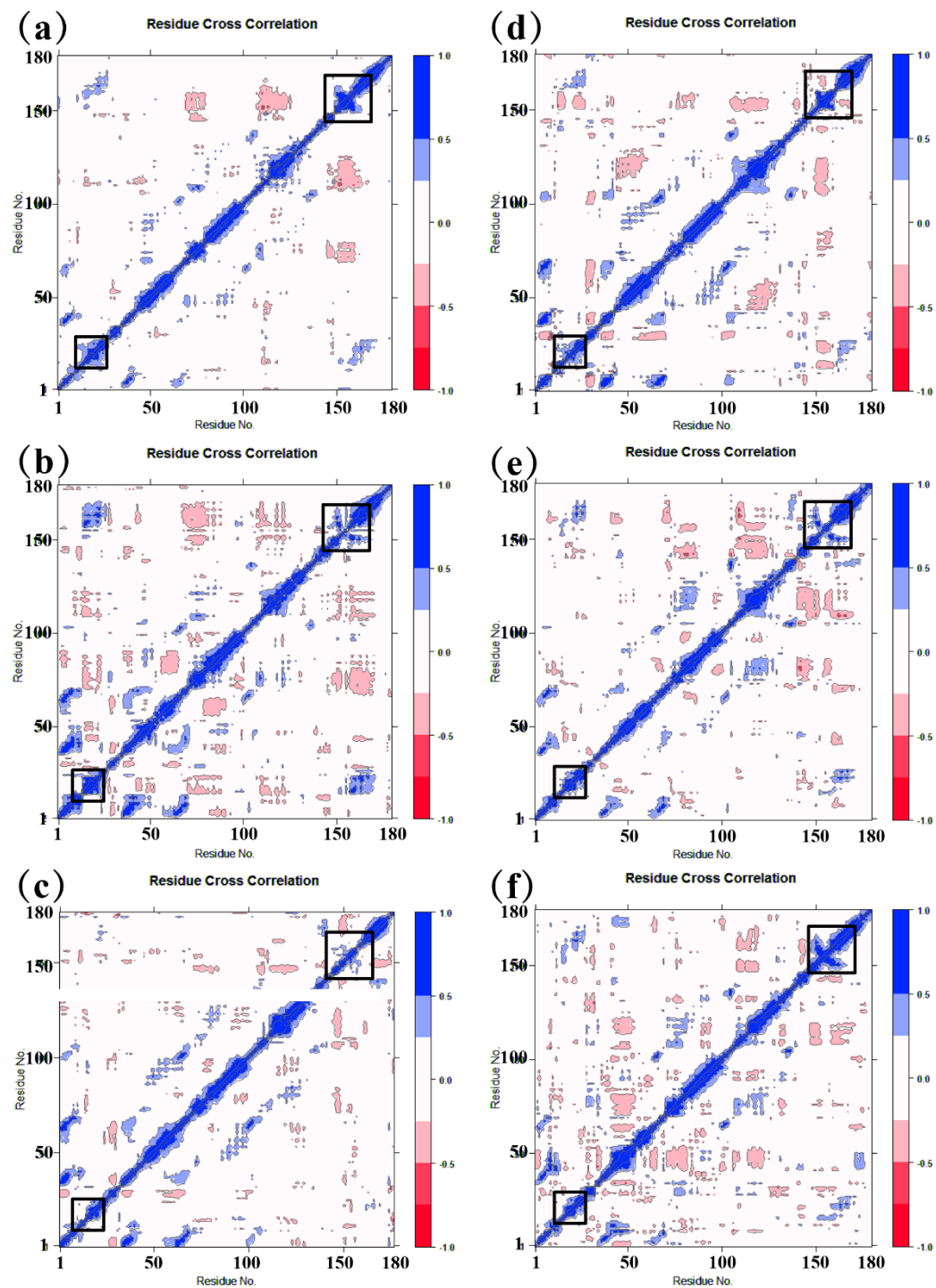


Figure S5. Cross-correlation matrix maps for the six complexes. (a) 'TesA_C16-SNAC; (b) 'TesA^{E142D/Y145G}_C16-SNAC; (c) 'TesA^{M141L/E142D/Y145G}_C16-SNAC; (d) 'TesA_C8-SNAC; (e) 'TesA^{E142D/Y145G}_C8-SNAC, and (f) 'TesA^{M141L/E142D/Y145G}_C8-SNAC.

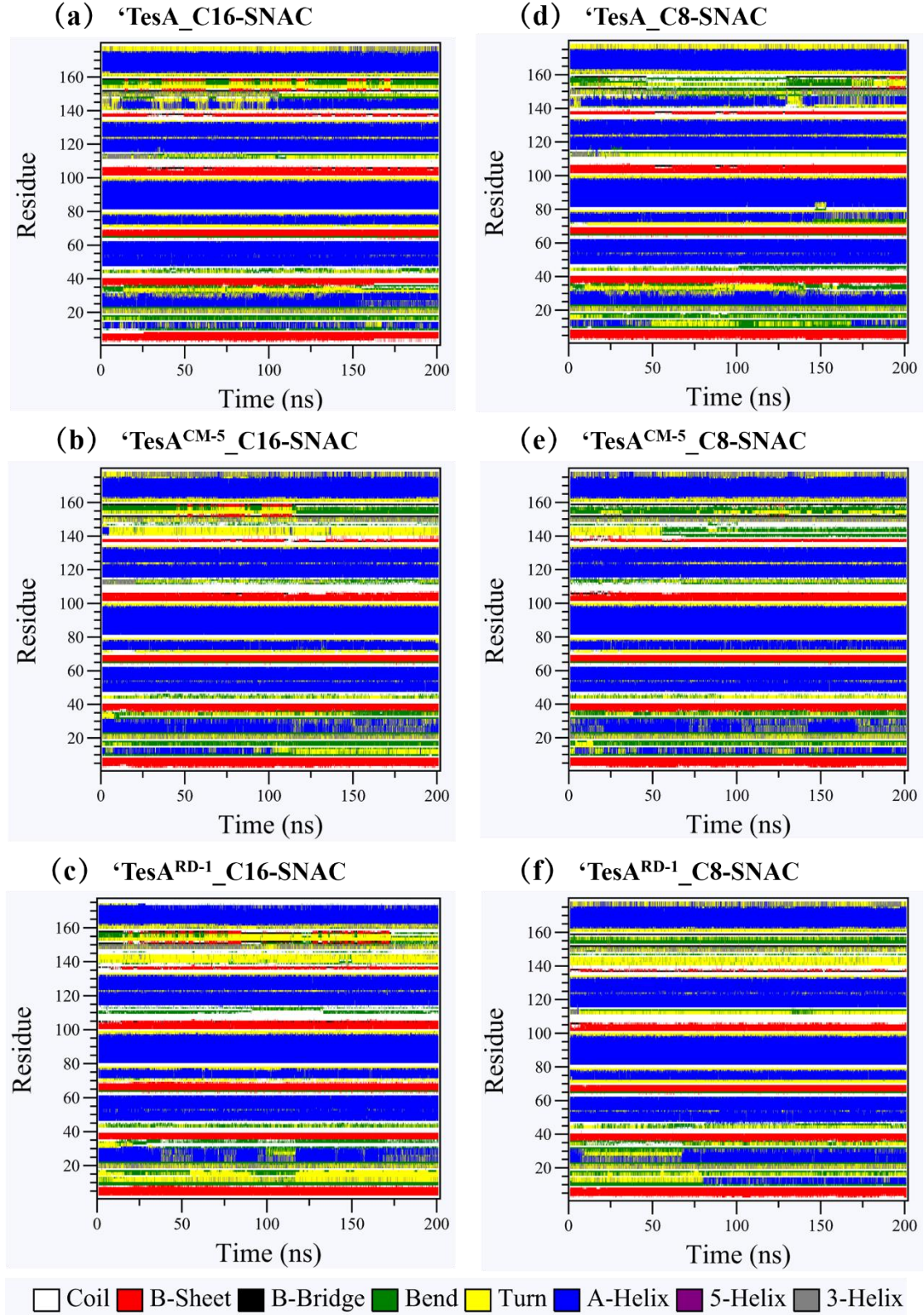


Figure S6. Comparison the differences of the secondary structures of the six complexes. (a) 'TesA_C16-SNAC, (b) 'TesA^{E142D/Y145G}_C16-SNAC, (c) 'TesA^{M141L/E142D/Y145G}_C16-SNAC, (d) 'TesA_C8-SNAC, (e) 'TesA^{E142D/Y145G}_C8-SNAC, (f) 'TesA^{M141L/E142D/Y145G}_C8-SNAC.

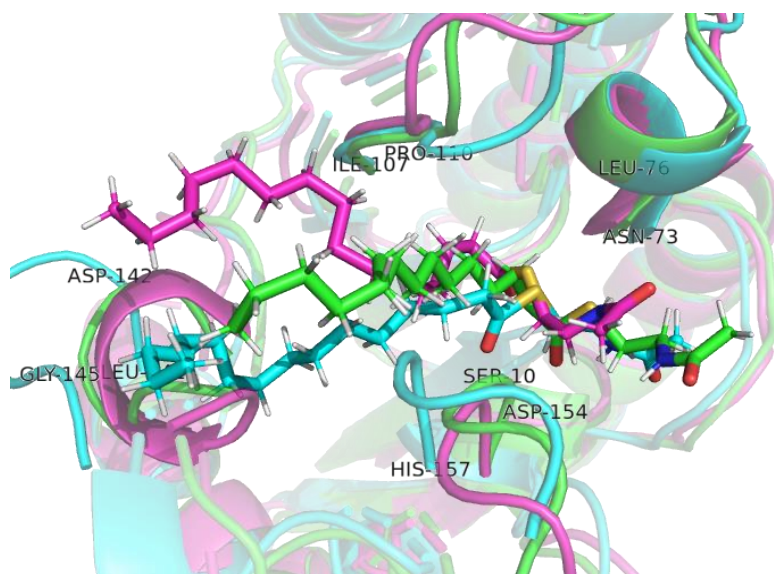


Figure S7. Schematic representation of the interaction pattern of long-chain substrate complexes. 'Tesa_C16-SNAC is shown in pink, 'Tesa^{E142D/Y145G}_C16-SNAC is shown in green, 'Tesa^{M141L/E142D/Y145G}_C16-SNAC is shown in blue.

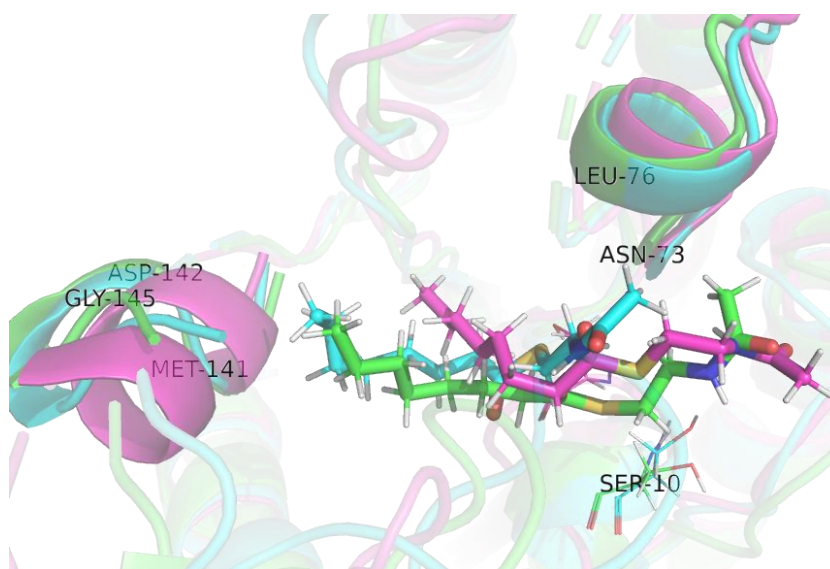


Figure S8. Schematic representation of the interaction pattern of medium-chain substrate complexes. 'Tesa_C8-SNAC is shown in pink, 'Tesa^{E142D/Y145G}_C8-SNAC is shown in green, 'Tesa^{M141L/E142D/Y145G}_C8-SNAC is shown in blue.

Table S1. The decomposition energies of the important residues.

(a). The decomposition energies of the important residues in 'TesA_C16-SNAC. (kJ/mol)

| Residues | Ser10 | Leu11 | Gly72 | Asn73 | Ile107 | Arg108 | Leu109 |
|-------------------|---------|---------|---------|----------|---------|---------|---------|
| ΔE_{MM} | -5.4113 | -6.9677 | -6.0569 | -16.5991 | -1.7039 | -6.6693 | -5.8468 |
| ΔG_{bind} | 1.5209 | -6.2565 | -2.6567 | -7.3644 | -1.8955 | 1.2032 | -2.1816 |
| Residues | Pro110 | Met141 | Glu142 | Tyr145 | Leu146 | Ile156 | His157 |
| ΔE_{MM} | -6.1506 | -7.4181 | -6.6864 | -8.7848 | -2.5326 | -7.5465 | -5.6473 |
| ΔG_{bind} | -4.4578 | -4.2467 | -0.2425 | -7.4043 | -2.6918 | -3.7862 | 0.6175 |

 $(\Delta E_{MM} = \Delta G_{vdw} + \Delta G_{elec})$ (b). The decomposition energies of the important residues in 'TesA^{E142D/Y145G}_C16-SNAC. (kJ/mol)

| Residues | Leu11 | Asn73 | Leu109 | Pro110 | Leu146 | Met151 | Ile156 | His157 |
|-------------------|---------|---------|---------|---------|---------|---------|---------|----------|
| ΔE_{MM} | -2.6399 | -2.8877 | -2.8893 | -3.6327 | -4.0013 | -3.0215 | -8.6553 | -13.3023 |
| ΔG_{bind} | -2.0474 | -1.5397 | -1.2238 | -2.763 | -2.3213 | -2.6766 | -3.5982 | -4.2147 |

(c). The decomposition energies of the important residues in 'TesA^{M141L/E142D/Y145G}_C16-SNAC. (kJ/mol)

| Residues | Asp9 | Ser10 | Ser43 | Asn73 | Pro110 | Phe139 | Ile156 | His157 |
|-------------------|---------|---------|--------|---------|---------|---------|---------|---------|
| ΔE_{MM} | -2.1352 | -1.7101 | -1.523 | -3.2806 | -2.322 | -0.9367 | -2.4828 | -0.9735 |
| ΔG_{bind} | -0.1302 | 0.4375 | 0.7762 | -0.8732 | -1.9267 | -0.8993 | -0.7559 | -0.2634 |

(d). The decomposition energies of the important residues in 'TesA_C8-SNAC. (kJ/mol)

| Residues | Ser10 | Leu11 | Asn73 | Leu76 | Arg77 | Ile107 | Tyr113 | Ile156 | His157 |
|-------------------|---------|---------|---------|---------|----------|---------|---------|---------|---------|
| ΔE_{MM} | -1.6902 | -2.4458 | -4.6137 | -3.6435 | -10.1425 | -0.9886 | -3.8976 | -4.5521 | -4.3856 |
| ΔG_{bind} | 0.9813 | -2.3301 | 0.5148 | -3.2844 | -2.5205 | -1.0713 | -0.5999 | -2.827 | 0.5589 |

(e). The decomposition energies of the important residues in 'TesA^{E142D/Y145G}_C8-SNAC. (kJ/mol)

| Residues | Ser10 | Leu11 | Asn73 | Leu76 | Ile107 | Phe139 | Phe140 |
|-------------------|---------|---------|---------|---------|----------|----------|---------|
| ΔE_{MM} | -7.056 | -4.9327 | -6.5819 | -1.2222 | -3.7896 | -3.7896 | -8.7479 |
| ΔG_{bind} | -2.5499 | -5.1396 | 2.4673 | -1.9206 | -1.4419 | -3.3596 | -6.6385 |
| Residues | Met141 | Leu146 | Trp150 | Met151 | Ile156 | His157 | Pro158 |
| ΔE_{MM} | -2.4057 | -4.8823 | -6.7299 | -4.8235 | -10.8587 | -13.0054 | -7.5239 |
| ΔG_{bind} | -1.9558 | -3.9712 | -3.3766 | -4.2767 | -3.5096 | -6.7304 | -5.804 |

(f). The decomposition energies of the important residues in 'TesA^{M141L/E142D/Y145G}_C8-SNAC. (kJ/mol)

| Residues | Asp9 | Ser10 | Leu11 | Asn73 | Leu76 | Arg77 | Ile107 |
|-------------------|---------|---------|---------|----------|----------|----------|---------|
| ΔE_{MM} | -5.618 | -7.8027 | -4.0408 | -10.0613 | -5.6674 | -3.7896 | -8.7479 |
| ΔG_{bind} | 1.6933 | -3.2924 | -3.2269 | -3.9608 | -5.1294 | -3.3596 | -6.6385 |
| Residues | Phe139 | Phe140 | Met141 | Gly155 | Ile156 | His157 | Pro158 |
| ΔE_{MM} | -2.1692 | -2.3081 | -1.1016 | -6.654 | -17.5376 | -12.8284 | -4.4256 |
| ΔG_{bind} | -1.5028 | -1.7411 | -0.7074 | -3.6624 | -7.0885 | -1.4851 | -2.0698 |